Bull. Chem. Soc. Ethiop. **2024**, 38(6), 1827-1842.
DOI: https://dx.doi.org/10.4314/bcse.v38i6.25

ISSN 1011-3924
Printed in Ethiopia
Online ISSN 1726-801X

SYNTHESIS, CHARACTERIZATION, DENSITY FUNCTIONAL THEORY (DFT) ANALYSIS, AND MESOMORPHIC STUDY OF NEW THIAZOLE DERIVATIVES

Sardasht Rifaat Taher[1,2*] and Wali Mahood Hamad[1]

[1]Department of Chemistry, Faculty of Science and Health, Koya University, Iraq
[2]Department of Petroleum Technology - Chemical Analysis, Koya Technical Institute, Erbil Polytechnic University, Iraq

(Received March 8, 2024; Revised June 6, 2024; Accepted June 13, 2024)

ABSTRACT. This study focuses on synthesizing and characterizing a new series of organic compounds with a heterocyclic core based on sulfur (thiazole). These compounds, labeled as N-(4-(4-alkoxyphenyl) thiazol-2-yl)-1-(naphthalen-2-yl) methanimine (ATNM)n, incorporate alkoxy chains of varying lengths ($C_nH_{2n+1}O$, n = 2, 3, 4, 5, 6, 7, 8, 9, 10, and 12) through a multi-step process. Structural analysis using FT-IR, ^{1}H-NMR, and ^{13}C-NMR confirmed the composition of these compounds. Theoretical calculations using density functional theory (DFT) were carried out with the B3LYP 6-311G (d,p) basis set for the entire set of synthesized compounds (ATNM)n. The (Gaussian 9) software was employed to compute optimized geometrical structures of the proposed compounds in the gas phase. However, investigations into their phase behavior using polarizing optical microscopy (POM) and differential scanning calorimetry (DSC) revealed that none of the compounds in this series exhibited the typical mesomorphic characteristics of liquid crystals. Comparisons were made between theoretical predictions from DFT and observed data obtained through synthesized compounds study. The results revealed that the presence of terminal alkoxy significantly influenced the overall energy of potential geometric structures, along with their physical and thermal characteristics.

KEY WORDS: Heterocyclic compounds, Thiazole, Liquid crystals, DFT, Methanimine

INTRODUCTION

Liquid crystals represent a distinctive state of matter, displaying characteristics of both liquids and crystals. While their molecular arrangement mirrors the order found in crystals, their fluid-like molecular structure is close to that of liquids. This distinctive blend of attributes gives rise to fascinating optical, electrical, and mechanical phenomena [1]. Heterocyclic compounds, on the other hand, are organic compounds featuring at least one ring structure in which one or more of the atoms within the ring are elements other than carbon, such as nitrogen, oxygen, or sulfur. The size and configuration of these heterocyclic moiety vary, playing a crucial role in determining the properties and behavior of liquid crystal materials [2]. Heterocyclic liquid crystals constitute a category of liquid crystals constructed from heterocyclic (ring-shaped) molecules as their fundamental units [3]. Thiazole liquid crystals, on the other hand, represent a subset of liquid crystalline compounds featuring thiazole rings in their molecular architecture [4]. Thiazole, a five-membered heterocyclic compound, comprises three carbon atoms, one nitrogen atom, and one sulfur atom in its ring structure, denoted by the molecular formula (C_3H_3NS). Recognized for its aromatic properties, thiazole is commonly present in diverse natural and synthetic compounds, including pharmaceuticals and agrochemicals, owing to its distinctive electronic and structural characteristics [5]. Thiazole-derived compounds are prepared through diverse methodologies, including the Hantzsch synthesis [6], Gewald reaction [7], or Vilsmeier-Haack reaction [8]. In the Hantzsch synthesis, for instance, thiazoles can be synthesized by combining α-haloketones with thiourea or thioamides in the presence of a base [6].

When integrated into liquid crystal compounds, the inclusion of thiazole rings can impact the overall characteristics and performance of the liquid crystal material. This influence extends to

*Corresponding authors. E-mail: sardasht.taher@epu.edu.iq

factors such as polarity and polarizability, the angle of rotations between molecular fragments, temperatures associated with phase transitions, Involvement in intermolecular interactions, determination of the mesophase type, modulation of the direction and magnitude of the dipole moment constant within the molecules, and the potential alteration of the sign and magnitude of the liquid crystal's dielectric anisotropy [9]. Thiazole rings possess aromatic and planar characteristics, exhibiting higher aromaticity compared to their oxazole counterparts due to more extensive pi-electron delocalization. The specific tile geometry of the thiazole ring connected to the benzene azomethine group plays a crucial role in liquid crystals, contributing to enhanced mesomorphic properties over a broad temperature range. Numerous research endeavors have explored the liquid crystalline traits of azomethines featuring thiazole rings. Recent studies have involved the synthesis of novel azomethines incorporating thiazole rings and liquid crystals with a bent-rod structure characterized by lengthy alkoxyl chains. Kuvatov and coworkers have conducted research on a series of liquid crystals, incorporating a thiazole ring with various terminal substituents [10].

Murza and coworkers successfully created a series of liquid crystals, specifically azomethines, denoted as 2-(4-alkoxybenzylideneamino)-4-(3-nitrophenylamino) thiazoles. The series encompasses various alkoxy chain lengths ($C_nH_{2n+1}O$, with n ranging from 1 to 10). Interestingly, every member within this series exhibits mesomorphism in the temperature range of 42-137 °C [11]. Moreover, Karam and collaborators have synthesized and investigated the liquid crystalline characteristics of a compound series featuring thiazole rings with diverse terminal groups, including amides, alkoxy series, ester, and azo linkage. The majority of compounds in this series demonstrate nematic (N) and smectic C (SmC) mesomorphism, with only two exceptions that do not exhibit liquid crystalline properties [12]. Additionally, Karam and coworkers have developed novel symmetrical and non-symmetrical mesogenic compounds incorporating thiazole rings, comprising homologous series with terminal alkoxy substituents. All compounds display liquid crystalline properties characterized by an anisotropic nematic mesophase except for the final homologue (n=8), which transitions to an isotropic liquid [13]. In this research, we describe the synthesis, characterization, (DFT), and mesomorphic behavior of newly synthesized compounds incorporating thiazole rings and possessing different lengths of alkoxy chains as terminal groups.

EXPERIMENTAL

Materials

Bromo alkanes [bromo (ethane, propane, butane, pentane hexane heptane, octane, nonane, decane, and dodecane)]: Sigma - Aldrich, Germany; iodine: Bio Chemo Pharma, France; thiourea: Bio Chemo Pharma; 4-hydroxyacetophenone: Sigma - Aldrich, Germany; anhydrous potassium carbonate: Scahrlau, Belgium; diethyl ether: Scahrlau, Belgium; chloroform: Scahrlau, Belgium; acetone: Bio Chemo Pharma, France; piperidine: Sigma - Aldrich, Germany; tetrahydrofuran: Bio Chemo Pharma, France; absolute ethanol (99%): Supelco, Germany; ammonia solution (25%): Bio Chemo Pharma, France; 2-naphthaldehyde: Sigma - Aldrich, Germany; silica gel for column chromatography: Bio Chemo Pharma, France. All required chemicals (reagents and solvents) were used directly without further purification.

Techniques

The melting points were measured with a Buchi Germany Model.B-540 electrothermal melting point apparatus. Infrared spectra were captured using an FT-IR Shimadzu 1S. ^{1}H NMR and ^{13}C NMR spectra were acquired with a Bruker spectrometer (400 MHz) in $CDCl_3$ as a solvent, using tetramethyl silane (TMS) as an internal standard. Chemical shifts were reported in δ (ppm) units, indicating multiplicity with standard expressions (singlet(s), doublet (d), triplet(t), multiplet (m),

coupling constant (*J*), and Hertz (Hz)). For the investigation of phase transitions and mesomorphic textures, a polarized optical microscopy (OPtika B-383POL, Italy) was employed. This was coupled to an MHCS400 hot and cold stage, configured with an MTDC600 temperature controller (temperature range: 25-400 °C), from Microptika, Netherlands. Additionally, an OPtika C-B18 USB Camera (18Mp, Italy) was used for imaging. Thermal transitions and enthalpies were determined through DSC measurements using a DSC 204 F1 Phoenix, NETZCH, Germany, equipped with a cooling system. The measurements were conducted at a heating/cooling rate of 10 °C min^{-1}, with a nitrogen flow of 50 mL min^{-1}.

All computations for the analyzed derivatives were performed utilizing Gaussian 09 software [14, 15] on a personal computer with a Core i7, 9th generation processor. The calculations were carried out employing DFT/B3LYP methods and a 6-311G (d,p) basis set. Optimization of geometries involved minimizing energies concerning all geometric parameters, without enforcing any molecular symmetry constraints. Visualization of the optimized geometries was facilitated using Gauss view. Additionally, frequency calculations were conducted at the same level of theory. The results from the frequency calculations indicated that all structures served as stationary points in the geometry optimization procedures, and none exhibited imaginary frequencies during the vibrational analyses. Assignments of vibrational modes were made through visual examination of the animated modes using the Gauss view program [16, 17].

Synthesis

Preparation of 4-(2-aminothiazol-4-yl) phenol (i)

A mixture containing (13.6 g, 0.1 mol of 4-hydroxy acetophenone (1-(4-hydroxyphenyl) ethan-1-one), (15.22 g, 0.2 mol of thiourea), and (25.31 g, 0.1 mol of iodine) was heated in a (250 mL) round bottom flask on a steam-bath overnight. After cooling, the crude reaction mixture was extracted with diethyl ether to eliminate unreacted (1-(4-hydroxyphenyl) ethan-1-one) and iodine. The resulting residue was dissolved in boiling water, followed by filtration to eliminate sulfur. The solution was then partially cooled and rendered basic using concentrated ammonium hydroxide. The (4-(2-aminothiazol-4-yl) phenol) separated out and was subsequently subjected to recrystallization from a mixture of water and alcohol [18].

Preparation of 4-(4-alkoxyphenyl) thiazol-2-amine (ii)

In a round-bottom flask (50 mL) equipped with a reflux condenser, a mixture comprising (0.28 g, 1.5 mmol) of 4-(2-aminothiazol-4-yl) phenol (i), (0.8 g, 2 mmol) of anhydrous potassium carbonate, (20 mL) of dry acetone, and (4 mmol) of n-bromoalkane was introduced. The mixture was then refluxed overnight. Subsequently, the resulting mixture was poured onto ice water, and the precipitate was filtered, washed with water, dried, and subjected to recrystallization using ethanol [19].

Synthesis of N-(4-(4-alkoxyphenyl) thiazol-2-yl)-1-(naphthalen-2-yl) methenamine (ATNM)n (iii)

A quantity of (0.042 mol) of 4-(4-alkoxyphenyl) thiazol-2-amine (ii), along with (0.042 mol, 6.55 g) of 2-naphthaldehyde, and (20 mL) of tetrahydrofuran (THF), containing a catalytic amount of piperidine (1-4 drops), were combined in a round-bottom flask (50 mL) equipped with a reflux condenser. The mixture was then refluxed for a duration of 4 hours. Upon completion of the reflux, the solvent was evaporated, and the resulting residue (ATNM)n (iii) was extracted using diethyl ether. The extract was subsequently purified through column chromatography using mixture of ethyl acetate and n-hexane as eluent with the ratio of (3:7) [20].

A compound N-(4-(4-ethoxyphenyl) thiazol-2-yl)-1-(naphthalen-2-yl) methenamine (ATNM)2 has a yield: (60%). M.P. 139 °C. IR (cm^{-1}) aromatic (C-H) str.3105.39, aliphatic (C-H) str. 2956.87 - 2856.58, (C=N thiazole) str. 1646, (C=N Schiff base imine) str. 1606.7, (C=C) str. 1577.77, (C-S) str. 661.58, (C-O-C alkoxy) str. 1251.180 - 1163.08 [21]. The ^{1}H NMR (400 MHz, $CDCl_3$) ppm (δ H): 9.21 (s, 1H, H11), 8.33 (s, 1H, H14,) [22], 8.24 - 8.22 (d, *J* = 8.0 Hz, 1H, H7), 7.96 - 7.84 (m, 6H, H1, 2, 4, 5, 9, 10), 7.61 - 7.53 (m, 2H, H16), 6.97 - 6.95 (d, *J* = 8.8 Hz, 2H, H17) [23], 4.11 - 3.95 (m, 2H, H21), 1.34 - 1.30 (t, *J* = 6.8 Hz, 3H, H22). In the ^{13}C NMR (100 MHz, $CDCl_3$) ppm (δ C): 172.30 (C12), 163.34 (C14), 159.33 (C18), 153.77 (C13), 135.64 (C3), 133.30 (C8), 128.89 (C6), 128.29 (C4), 128.04 (C2, 9, 16, 20), 127.20 (C7), 126.85 (1,10), 126.23(C21), 124.15 (C15), 114.66 (C17, 19), 110.02 (C14), 69.59 (C21), 14.8 (C22, CH_3). The color of the product is light yellow.

A compound of 1-(naphthalen-2-yl)-N-(4-(4-propoxyphenyl) thiazol-2-yl) methanimine (ATNM)3 has a yield: (66%). M.P. 171.9 °C. IR (cm^{-1}) aromatic (C-H) str. 3105.39, aliphatic (C-H) str. 2956.87 - 2856.58, (C=N thiazole) str. 1646, (C=N Schiff base imine) str. 1606.7, (C=C) str. 1577.77, (C-S) str. 661.58, (C-O-C alkoxy) str. 1251.180 - 1163.08. The ^{1}H NMR (400 MHz, $CDCl_3$) ppm (δ H): 9.21 (s, 1H, H11), 8.33 (s, 1H, H14), 8.24 - 8.22 (d, *J* = 8.0 Hz, 1H, H7), 7.96 - 7.84 (m, 6H, H1, 2, 4, 5, 9, 10), 7.61 - 7.53 (m, 2H, H16), 6.97 - 6.95 (d, *J* = 8.8 Hz, 2H, H17), 3.98 - 3.95 (t, *J*= 6.6 Hz, 2H, H21), 1.88 - 1.79 (m, 2H, H22), 1.08 - 1.04 (t, *J* = 6.8 Hz, 3H, H23). In the ^{13}C NMR (100 MHz, $CDCl_3$) ppm (δ C): 172.30 (C12), 163.34 (C14), 159.33 (C18), 153.77 (C13), 135.64 (C3), 133.30 (C8), 128.89 (C6), 128.29 (C4), 128.04 (C2, 9, 16, 20), 127.20 (C7), 126.85 (C1,10), 126.23 (C21), 124.15 (C15), 114.66 (C17, 19), 110.02 (C14), 69.59 (C21), 22.63 (C22), 10.58 (C23). The color of the product is yellow.

A compound of N-(4-(4-butoxyphenyl) thiazol-2-yl)-1-(naphthalen-2-yl) methanimine (ATNM)4 has a yield: (69%). M.P. 91.9 °C. IR (cm^{-1}) aromatic (C-H) str. 3103.46, aliphatic (C-H) str. 2956.87 - 2856.58, (C=N thiazole) str. 1646, (C=N Schiff base imine) str. 1608.63, (C=C) str. 1577.62, (C-S) str. 655.680, (C-O-C alkoxy) str. 1253.73 - 1163.16. The ^{1}H NMR (400 MHz, $CDCl_3$) ppm (δ H): 9.16 (s, 1H, H11), 8.27 (s, 1H, H14), 8.22 - 8.20 (d, *J* = 8.0 Hz, 1H, H7), 7.92 - 7.81 (m, 6H, H1, 2, 4, 5, 9, 10), 7.58 - 7.50 (m, 2H, H16), 6.95 - 6.93 (d, *J* = 8.4 Hz, 2H, H17), 3.98 - 3.95 (t, *J* = 6.6 Hz, 2H, H21), 1.82 - 1.75 (m, 2H, H22), 1.46 - 1.42 (m, 2H, H23), 0.95 - 0.92 (t, *J*= 6.8 Hz, 3H, H24). In the ^{13}C NMR (100 MHz, $CDCl_3$) ppm: (δ C) 172.29 (C12), 163.36 (C11), 159.35 (C18), 153.76 (C13), 135.63 (C3), 133.30 (C8), 128.88 (C6), 128.28 (C4), 128.03 (C2, 9, 16, 20), 127.20 (C7), 126.85 (C1,10), 126.23 (C21), 124.15 (C15), 114.67 (C17, 19), 110.03 (C14), 68.09 (C21), 29.03 (C22), 22.54 (C23), 14.00 (C24). The color of the product is yellow.

A compound of 1-(naphthalen-2-yl)-N-(4-(4-(pentyloxy) phenyl) thiazol-2-yl) methenamine (ATNM)5 has a yield: (70%). M.P. 171.8 °C. IR (cm^{-1}) aromatic (C-H) str. 3101.54, aliphatic (C-H) str. 2933.73 - 2854.65, (C=N) str. 1646.63, (C=N Schiff base imine) str. 1608.63, (C=C) str. 1529.55, (C-S) str. 655.680, (C-O-C alkoxy) str. 1255.66 - 1161.15. The ^{1}H NMR (400 MHz, $CDCl_3$) ppm (δ H): 9.16 (s, 1H, H11), 8.27 (s, 1H, H14), 8.22 - 8.20 (d, *J* = 8.0 Hz, 1H, H7), 7.92 - 7.81 (m, 6H, H1, 2, 4, 5, 9, 10), 7.58 - 7.50 (m, 2H, H16), 6.95 - 6.93 (d, *J* = 8.4 Hz, 2H, H17), 3.98 - 3.95 (t, *J* = 6.6 Hz, 2H, H21), 1.82 - 1.75 (m, 2H, H22), 1.46 - 1.44 (m, 4H, H23, 24), 0.95 - 0.92 (t, *J*= 6.8 Hz, 3H, H25). In the ^{13}C NMR (100 MHz, $CDCl_3$) ppm (δ C): 172.29 (C12), 163.36 (C11), 159.35 (C18), 153.76 (C13), 135.63 (C3), 133.30 (C8), 128.88 (C6), 128.28 (C4), 128.03 (C2, 9, 16, 20), 127.20 (C7), 126.85 (C2), 126.23 (C1,10), 124.15 (C15), 114.67 (C17, 19), 110.03 (C14), 68.09 (C21), 29.03 (C22), 28.26(C23), 22.54 (C24), 14.00 (C25). The color of the product is yellow.

A compound of N-(4-(4-(hexyloxy) phenyl) thiazol-2-yl)-1-(naphthalen-2-yl) methanimine

(ATNM)6 has a yield: (74%). M.P. 166.8 °C. IR (cm^{-1}) aromatic (C-H) str. 3103.48, aliphatic (C-H) str. 2933.73 - 2856.58, (C=N thiazole) str. 1646, (C=N Schiff base imine) str. 1608.63, (C=C) str. 1529.55, (C-S) str. 661.58, (C-O-C alkoxy) str. 1253.73 - 1161.15. The ^{1}H NMR (400 MHz, $CDCl_3$) ppm (δ H): 9.16 (s, 1H, H11), 8.27 (s, 1H, H14), 8.22 - 8.20 (d, *J* = 8.0 Hz, 1H, H7), 7.92 - 7.81 (m, 6H, H1, 2, 4, 5, 9, 10), 7.58 - 7.50 (m, 2H, H16), 6.95 - 6.93 (d, *J* = 8.4 Hz, 2H, H17), 3.98 - 3.95 (t, *J* = 6.8 Hz , 2H, H21), 1.82 - 1.75 (m, 2H, H22), 1.46 - 1.29 (m, 6H, H23, 24, 25), 0.91 - 0.88 (t, *J* = 6.8 Hz, 3H, H26). In the ^{13}C NMR (100 MHz, $CDCl_3$) ppm (δ C): 172.28 (C12), 163.28 (C11), 59.35 (C18), 153.63 (C13), 135.63 (C3), 133.28 (C8), 128.87 (C6), 128.27 (C4), 128.03 (C2, 9, 16, 20), 127.21 (C7), 126.84 (C2), 126.23 (C1,10) , 124.16 (C15), 114.68 (C17, 19) , 110.02 (C14), 68.11 (C21), 31.84 (C22), 29.14 (C23), 26.07 (C24), 22.68 (C24), 14.17 (C26). The color of the product is deep - yellow.

A compound of N-(4-(4-(heptyloxy) phenyl) thiazol-2-yl)-1-(naphthalen-2-yl) methanimine (ATNM)7 has a yield: (79%). M.P. 126.3 °C. IR (cm^{-1}) aromatic (C-H) str. 3103.46, aliphatic (C-H) str. 2953.16 - 2856.58, (C=N thiazole) str. 1646, (C=N Schiff base imine) str. 1608.63, (C=C) str. 1527.62, (C-S) str. 661.58, (C-O-C alkoxy) str. 1253.73 - 1161.15. The ^{1}H NMR (400 MHz, $CDCl_3$) ppm (δ H): 9.16 (s, 1H, H11), 8.28 (s, 1H, H14), 8.22 - 8.20 (d, *J* = 8.0 Hz, 1H, H7), 7.92 - 7.84 (m, 6H, H1, 2, 4, 5, 9, 10), 7.58 - 7.50 (m, 2H, H16), 6.95 - 6.93 (d, *J* = 8.4 Hz, 2H, H17), 3.98 - 3.95 (t, *J* = 6.8 Hz, 2H, H21), 1.82 - 1.75 (m, 2H, H22), 1.49 - 1.29 (m, 8H, H23, 24, 25,26), 0.91 - 0.88 (t, *J* = 6.8 Hz, 3H, H27). In the ^{13}C NMR (100 MHz, $CDCl_3$) ppm (δ C): 172.28 (C12), 163.28 (C11), 159.35 (C18), 153.63 (C13), 135.63 (C3), 133.28 (C8), 128.87 (C6), 128.27 (C4), 128.03 (C2, 9, 16, 20), 127.21 (C7), 126.84 (C2), 126.23 (C1,10), 124.16 (C15), 114.68 (C17, 19), 110.02 (C14), 68.11 (C21), 31.84 (C22), 29.34 (C23), 29.14 (C24), 26.07 (C25), 22.68 (C26), 14.11 (C27). The color of the product is deep - yellow.

A compound of 1-(naphthalen-2-yl)-N-(4-(4-(octyloxy) phenyl) thiazol-2-yl) methanimine (ATNM)8 has a yield: (82%). M.P. 120.6 °C. IR (cm^{-1}) aromatic (C-H) str. 3103.46, aliphatic (C-H) str. 2933.7 - 2850.72, (C=N thiazole) str. 1646, (C=N Schiff base imine) str. 1608.63, (C=C) str.1527.62, (C-S) str. 661.58, (C-O-C alkoxy) str. 1253.73 - 1161.15. The ^{1}H NMR (400 MHz, $CDCl_3$) ppm (δ H): 9.18 (s, 1H, H11), 8.29 (s, 1H, H14), 8.22-8.20 (d, *J* = 8.0 Hz, 1H, H7), 7.93 - 7.85 (m, 6H, H1, 2, 4, 5, 9, 10), 7.59 - 7.51 (m, 2H, H16), 6.96 - 6.94 (d, *J* = 8.4 Hz, 2H, H17), 3.99 - 3.96 (t, *J* = 7.0 Hz, 2H, H21), 1.82 - 1.75 (m, 2H, H22), 1.49 - 1.29 (m, 10H, H23, 24, 25,26, 27) , 0.91 - 0.88 (t, *J* = 6.8 Hz, 3H, H28). In the ^{13}C NMR (100 MHz, $CDCl_3$) ppm (δ C): 172.28 (C12), 163.28 (C11), 159.35 (C18), 153.78 (C13), 135.63 (C3), 133.26 (C8), 128.87 (C6), 128.26 (C4), 128.23 (C2, 9, 16, 20), 127.21 (C7), 126.84 (C2), 126.23 (C1,10), 124.16 (C15), 114.68 (C17, 19), 110.02 (C14), 68.11 (C21), 31.87 (C22), 29.43 (C23), 29.33 (C24), 29.14 (C25), 26.07 (C26), 22.68 (C27), 14.11 (C28). The color of the product is deep - yellow.

A compound of 1-(naphthalen-2-yl)-N-(4-(4-(nonyloxy) phenyl) thiazol-2-yl) methanimine (ATNM)9 has a yield: (83%). M.P. 129.9 °C. IR (cm^{-1}) aromatic (C-H) str. 3103.46, aliphatic (C-H) str. 2933.7 - 2850.72, (C=N thiazole) str. 1646, (C=N Schiff base imine) str. 1608.63, (C=C) str. 1527.62, (C-S) str. 663.51, (C-O-C alkoxy) str. 1253.73 - 1161.15. The ^{1}H NMR (400 MHz, $CDCl_3$) ppm (δ H): 9.19 (s, 1H, H11), 8.30 (s, 1H, H14), 8.22 - 8.20 (d, *J* = 8.0 Hz, 1H, H7), 7.94 -7.86 (m, 6H, H1, 2, 4, 5, 9, 10), 7.59 - 7.51 (m, 2H, H16), 6.96 - 6.94 (d, *J* = 8.4 Hz, 2H, H17), 4.00 - 3.96 (t, *J* = 6.4 Hz, 6.8, 2H, H21), 1.82 - 1.75 (m, 2H, H22), 1.46 - 1.28 (m, 12H, H23, 24, 25,26, 27, 28) , 0.91 - 0.88 (t, *J*= 6.63 Hz, 1H, H29). In the ^{13}C NMR (100 MHz, $CDCl_3$) ppm (δ C):172.28 (C12), 163.28 (C11), 159.36 (C18), 153.78 (C13), 135.63 (C3), 133.27 (C8), 128.87 (C6), 128.27 (C4), 128.23 (C2, 9, 16, 20), 127.21 (C7), 126.84 (C2), 126.23(C1,10), 124.16 (C15), 114.68 (C17, 19), 110.02 (C14), 68.12 (C21), 31.94 (C22), 29.61 (C23, 24, 25), 29.33 (C26), 26.10 (C27), 22.73 (C28), 14.11 (C29). The color of the product is deep - yellow.

A compound of N-(4-(4-(decyloxy) phenyl) thiazol-2-yl)-1-(naphthalen-2-yl) methanimine (ATNM)10 has a yield: (85%). M.P. 161.7 °C. IR (cm^{-1}) Aromatic (C-H) str. 3103.46, aliphatic (C-H) str. 2933.7 - 2848.86, (C=N thiazole) str. 1646, (C=N Schiff base imine) str. 1608.63, (C=C) str. 1529.55, (C-S) str. 663.51, (C-O-C alkoxy) str. 1253.73 - 1161.15. The ^{1}H NMR (400 MHz, $CDCl_3$) ppm (δ H): 9.19 (s, 1H, H11), 8.30 (s, 1H, H14), 8.22 - 8.20 (d, *J* = 8.0 Hz, 1H, H7) , 7.94 - 7.86 (m, 6H, H1, 2, 4, 5, 9, 10), 7.59 - 7.51 (m, 2H, H16), 6.96 - 6.94 (d, *J* = 8.4 Hz, 2H, H17), 4.00 - 3.96 (t, *J* = 6.8 Hz, 2H, H21), 1.82 - 1.75 (m, 2H, H22), 1.46 - 1.28 (m, 14H, H23, 24, 25,26, 27, 28, 29) , 0.91- 0.88 (t, *J* = 6.6 Hz, 3H, H30). In the ^{13}C NMR (100 MHz, $CDCl_3$) ppm (δ C): 172.28 (C12), 163.29 (C11), 159.36 (C18), 153.78 (C13), 135.63 (C3), 133.27 (C8), 128.87 (C6), 128.27 (C4), 128.23 (C2, 9, 16, 20), 127.21 (C7), 126.84 (C2), 126.24 (C1,10), 124.16 (C15), 114.68 (C17, 19), 110.01 (C14), 68.12 (C21), 31.94 (C22), 29.61 (C23, 24, 25, 26), 29.34 (C27), 26.05 (C28), 22.68 (C29), 14.12 (C30). The color of the product is yellow-orange.

A compound of N-(4-(4-(dodecyloxy) phenyl) thiazol-2-yl)-1-(naphthalen-2-yl) methanimine (ATNM)12 has a yield: (87%). M.P. 154.3 °C. IR (cm^{-1}) aromatic (C-H) str. 3105.39, aliphatic (C-H) str. 2918.30 - 2848.86, (C=N thiazole) str. 1646, (C=N Schiff base imine) str. 1608.63, (C=C) str. 1529.55, (C-S) str. 663.51, (C-O-C alkoxy) str. 1253.73 - 1163.08. The ^{1}H NMR (400 MHz, $CDCl_3$) ppm (δ H): 9.21 (s, 1H, H11), 8.33 (s, 1H, H14), 8.24 - 8.22 (d, *J* = 8.0 Hz ,1H, H7), 7.96- 7.88 (m, 6H, H1, 2, 4, 5, 9, 10), 7.61 - 7.54 (m, 2H, H16), 6.97 - 6.95 (d, *J*=8.4 Hz, 2H, H17), 4.01 - 3.98 (t, *J* = 6.8 Hz, 14.0, 7.2, 2H, H21), 1.82-1.76 (m, 2H, H22), 1.49 - 1.25 (m, 18H, H23, 24, 25,26, 27, 28, 29, 30, 31), 0.91 - 0.88 (t, *J* = 6.6 Hz, 3H, H32). In the ^{13}C NMR (100 MHz, $CDCl_3$) ppm (δ C): 172.27 (C12), 163.31 (C11), 159.36 (C18), 153.75 (C13), 135.61 (C3), 133.24 (C8), 128.87 (C6), 128.26 (C4), 128.00 (C2, 9, 16, 20), 127.27 (C7), 126.83 (C2), 126.24 (C1,10) , 124.12 (C15), 114.66 (C17, 19) , 110.01 (C14), 68.10 (C21), 31.94 (C22), 29.60 (C23, 24, 25, 26, 27, 28), 29.34 (C29), 26.05 (C30), 22.68 (C31), 14.12 (C32). The color of the product is yellow-orange.

RESULTS AND DISCUSSION

Synthesis

The iodination of 4-hydroxy acetophenone (1-(4-hydroxyphenyl) ethan-1-one) in present of thiourea results in the formation of 1-(4-hydroxyphenyl)-2-iodoethan-1-one. This compound can react with thiourea to produce 4-(2-aminothiazol-4-yl) phenol hydroiodide [24]. When this product is treated with anhydrous potassium carbonate (K_2CO_3) and subsequently reacted with an alkyl bromide (R-Br), it forms 4-(4-alkoxyphenyl) thiazol-2-amine. This amine then reacts with 2-naphthaldehyde to synthesize a series of ten N-(4-(4-alkoxyphenyl) thiazol-2-yl)-1-(naphthalen-2-yl) methenamines (ATNM)n [25], where n ranges from 2 to 10 and includes 12, as illustrated in Scheme 1.

Spectroscopic study

A series of (ATNM)n compounds was synthesized by combining equimolar quantities of compounds (i) and (ii) and subjecting the mixture to reflux in tetrahydrofuran (THF), with piperidine serving as a catalyst. Subsequently, the resulting mixtures underwent extraction using diethyl ether and purification via column chromatography. Initial characterization of these compounds involved FT-IR spectroscopy. The suitability of the proposed compositions for the investigated compounds was confirmed based on the outcomes obtained from infrared spectroscopy. The (ATNM)n configured compounds exhibited well-defined absorption bands, particularly at (1606 - 1608 cm^{-1}), corresponding to the stretching vibration of the azomethine (-C=N-) group (Schiff base imine) [26]. Additionally, distinct bands for ether (-C-O-C-) and (C-S) were observed in the range of (655.80 - 663.51 cm^{-1}) and (1251.18 -1161.15 cm^{-1}), respectively

[27]. The presence of (-C=N-) and (C-S) bands, coupled with the disappearance of amine (-NH_2) and carbonyl (C=O) absorption bands, respectively, indicates the formation of Schiff base derivatives (ATNM)n. Detailed structural information was elucidated through the analysis of ^{1}H-NMR and ^{13}C-NMR spectra. In the synthesis of compounds (ATNM)2-10 and 12, various alkoxy chain lengths were employed, resulting in yields ranging from 60% to 87%. The consistent alignment of physical properties, IR spectra, and NMR data for each compound with their respective structures provided valuable insights into their molecular characteristics. Notably, the diverse colors exhibited by the products, including light yellow, deep yellow, and yellow-orange, contribute an intriguing visual dimension to the overall study. Together, these results confirm the correct preparation of the synthesized compounds.

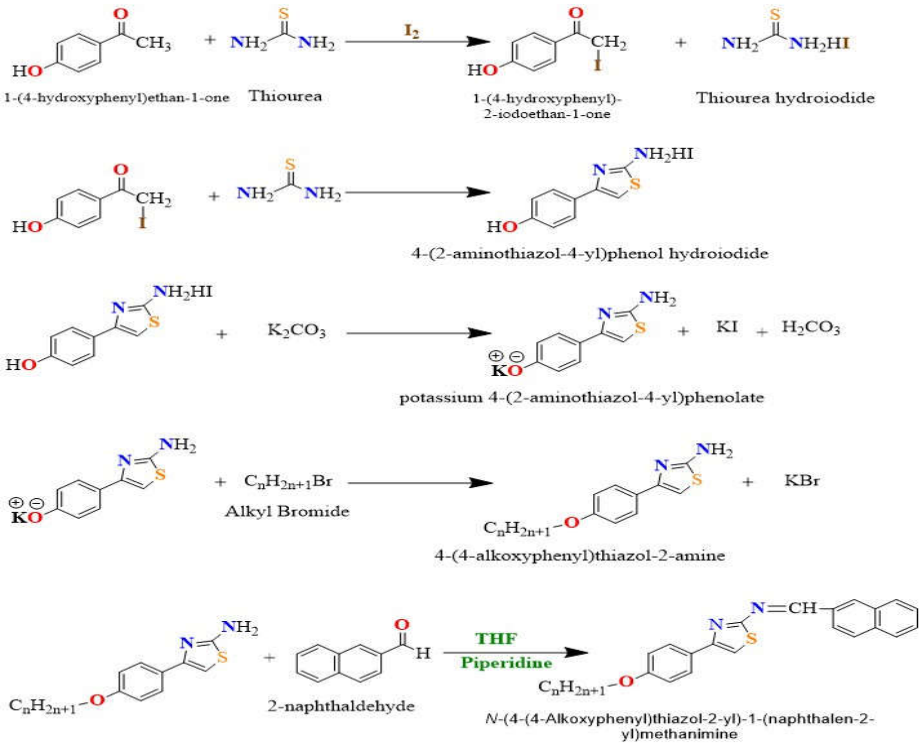

Scheme 1. Synthetic reactions, where (n = 2, 3, 4, 5, 6, 7, 8, 9, 10, and 12).

Thermal and microscopic characterization

Transition temperatures and mesophase types of all (ATNM)n series compounds were investigated using hot-stage polarizing optical microscopy (POM) and differential scanning calorimetry (DSC). In the DSC analysis, the compounds were subjected to heating and cooling cycles at a rate of 10 °C/min, ranging from 25 °C to approximately 50 °C above their melting points. The phase transitions were characterized by changes in enthalpy (ΔH) at specific transition temperatures [28]. Microscopy samples in this study were prepared by melting a small amount (4-5 mg) of the solid onto a clean and dry glass slide on the heating stage. Once the material had melted, an untreated glass coverslip was placed on top, creating a sandwich configuration with the sample between the glass surfaces [29]. The mesomorphic behavior of these samples was

identified, to the extent possible, based on their distinctive optical textures observed through polarized optical microscopy. This identification was achieved by comparing the observed textures with those documented in the existing literature [30].

The majority of liquid crystalline materials are widely recognized for their aromatic nature. Aromatic rings exhibited polarizability, planarity, and rigidity, and their structure can be fine-tuned by the strategic placement of substituents and linking units [31]. Organic molecules incorporating a naphthalene moiety, as opposed to a benzene moiety, typically contribute to an increased molecular breadth [32]. Despite the extensive knowledge about liquid crystals, fewer mesogenic derivatives of naphthalene have been thoroughly investigated, and only a limited number feature broad molecules with naphthalene units. The presence of naphthalene increases the breadth of the molecules, thereby reducing the thermal stabilities of the mesomorphic phase. [33].

None of the (ATNM)n series compounds examined through DSC and POM displayed any liquid crystalline behavior, as indicated in Table 1. The DSC thermograms of (ATNM)10 in Figure 1 reveal the absence of liquid crystalline mesophases, a conclusion supported by POM analysis (Figure 2). For this compound, the DSC depicts three transitions: the transition from the (Cr) phase to the (Cr_1) phase at (54 °C) with a transition enthalpy (ΔH) of (0.067 kJ/mol), the transition from (Cr_1) to (Cr_2) at (67 °C) with a transition enthalpy (ΔH) of (0.792 kJ/mol) and the transition from (Cr_2) to (I) at (67161.7 °C) with a transition enthalpy (ΔH) of (5.662 kJ/mol) Similarly, the DSC thermograms and POM textures for (ATNM)12 compound in Figure 3 and Figure 4 exhibit two transitions. The first corresponds to the transition from the (Cr) phase to the (Cr_1) phase at (95.5 °C) with a transition enthalpy (ΔH) of (1.307 kJ/mol), and the second is the transition from (Cr_1) to (I) at (154.3 °C) with a transition enthalpy (ΔH) of (5.002 kJ/mol).

Table 1. Transition temperature (°C) and molar enthalpy changes ΔH (kJ/mol) of (ATNM)n compounds.

Compound	Melting point (°C)	Transition temperature (°C) and ΔH (kJ/mol)
$(ATNM)_2$	139	Cr 139 (5.623) I
$(ATNM)_3$	171.9	Cr 171.9 (5.635) I
$(ATNM)_4$	91.9	Cr 91.9 (3.92) I
$(ATNM)_5$	171.8	Cr 171.8 (10.48) I
$(ATNM)_6$	166.8	Cr 166.8 (9.565) I
$(ATNM)_7$	126.3	Cr 126.3 (5.850) I
$(ATNM)_8$	120.6	Cr 120.6 (9.154) I
(ATNM)9	129.9	Cr 129.9 (10.14) I
(ATNM)10	161.7	Cr 54 (0.144) Cr_1 67 (0.792) Cr_2 161.7 (5.662) I
(ATNM) 12	154.3	Cr 95.5 (1.307) Cr_1 154.3 (5.002) I
Note: Cr = Crystal and I = Isotropic		

DFT and molecular geometries studies

Utilizing the DFT method, we estimated chemical quantum parameters and correlated them with experimental findings for the examined homologues (ATNM)n. In the current series, (ATNM)n did not exhibit liquid crystal (LC) properties, indicating a lack of a planar conformation. The stability of the optimized geometry for each member in the system was confirmed, as evidenced by the absence of imaginary frequencies in Figure 5. Table 2 consolidates all resulting energy and dipole moment parameters from the computational predictions. The anticipated polarity of the prepared compounds was observed to decrease with the length of the terminal chain, as indicated by the lower magnitude of the dipole moment with higher values of (n). This observation contradicts earlier reports [34] suggesting that the planarity of the mesogenic portion of LC

compounds is enhanced by the mesomorphic nature of the attached polar group. Consequently, the conjugated π-cloud interactions resulting from the oxygen atom of terminal alkoxy group provide high thermal stability with suitable geometrical parameters, deviating from the experimental findings in the present investigated series.

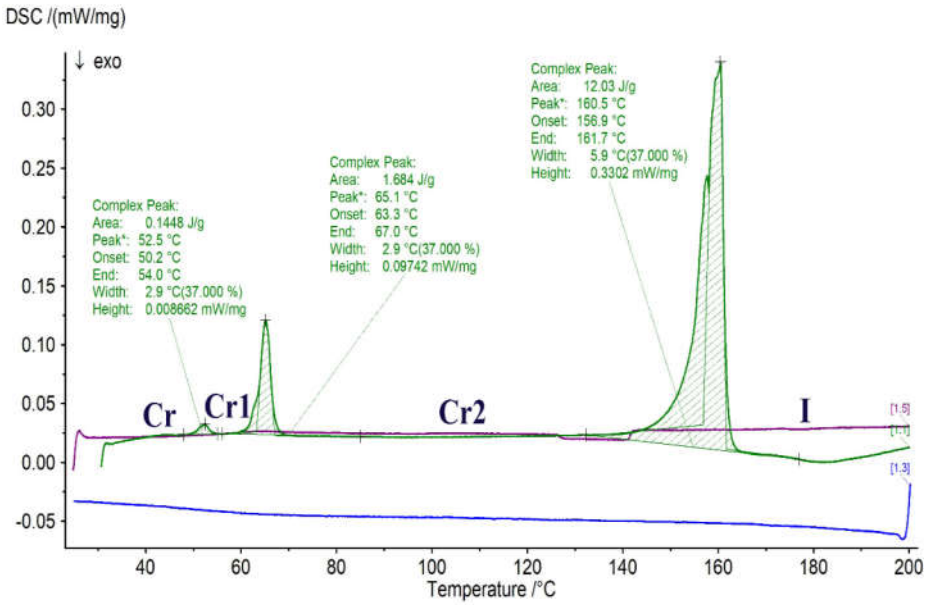

Figure 1. DSC thermogram of (ATNM)10 compound.

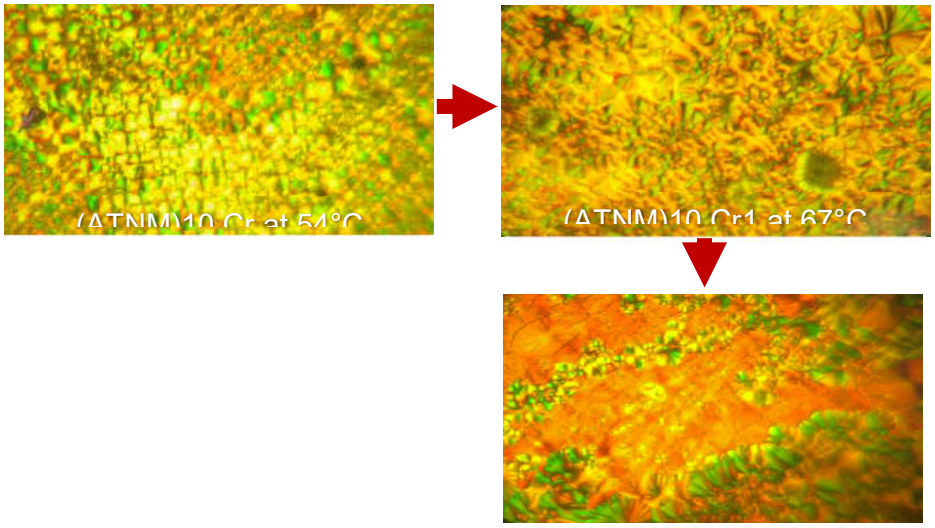

Figure 2. Textures of crystals under (POM) for (ATNM)10 compound.

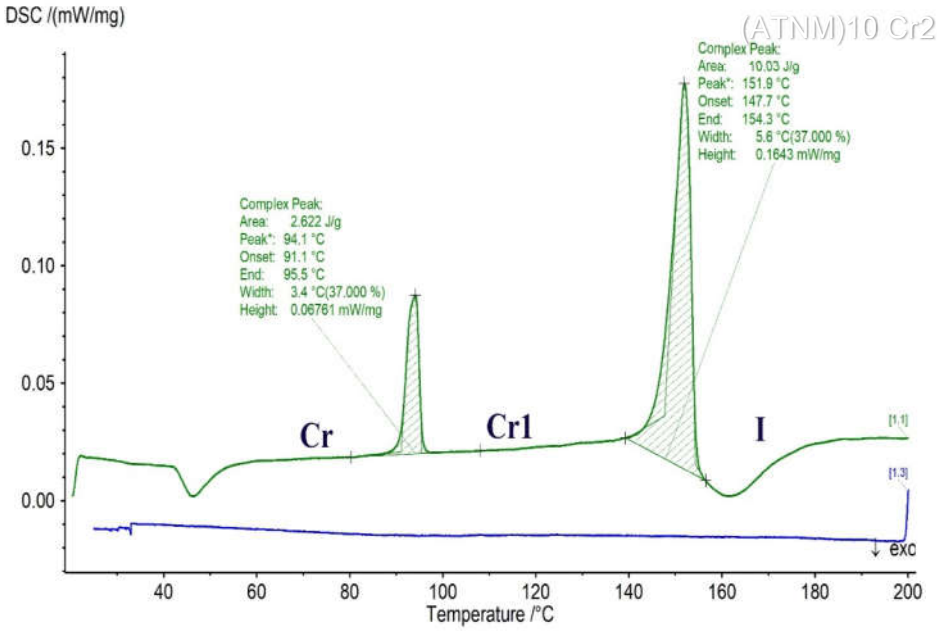

Figure 3. DSC thermogram of (ATNM)12 compound.

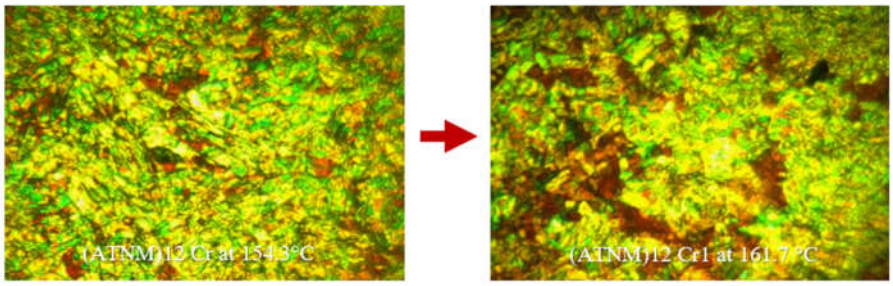

Figure 4. Textures of crystal under (POM) for (ATNM)12 compound.

Table 2. Total energy, dipole moment, and FMO energies (eV).

Compounds	Total energy (Hartree)	Dipole moment (Debye)	LUMO	HOMO	ΔE
(ATNM)2	-1432.372889	2.4026	-2.40	-5.50	3.10
(ATNM)3	-1471.697607	2.0099	-2.41	-5.49	3.09
(ATNM)4	-1511.021557	2.3303	-2.41	-5.50	3.09
(ATNM)5	-1550.345386	2.2268	-2.40	-5.49	3.09
(ATNM)6	-1589.669604	2.2743	-2.39	-5.48	3.09
(ATNM)7	-1628.9934934	2.0943	-2.39	-5.47	3.08
(ATNM)8	-1668.318031	2.2177	-2.39	-5.47	3.08
(ATNM)9	-1707.642253	2.1895	-2.39	-5.47	3.08
(ATNM)10	-1746.9661470	2.1611	-2.39	-5.47	3.08
(ATNM)12	-1825.607798	2.0699	-2.41	-5.48	3.07

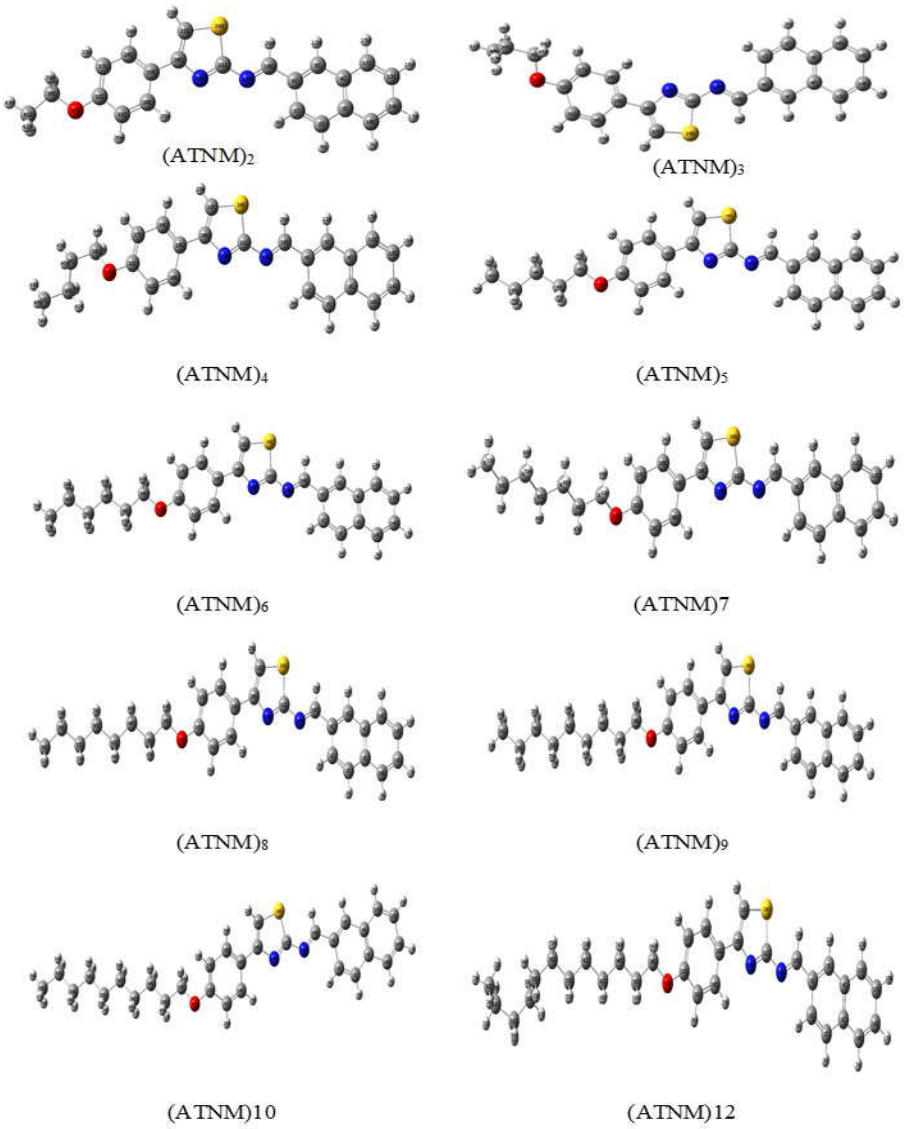

Figure 5. Calculated molecular optimized geometries of the synthesized (ATNM)n compounds.

Frontier molecular orbitals (FMOs)

Figure 6 illustrates the distribution of the highest occupied molecular orbital (HOMO) and lowest unoccupied molecular orbital (LUMO) for the (ATNM)n compounds synthesized in this study, as detailed in Table 2, which provides the corresponding energies and energy gaps. The energy gap (ΔE) between HOMO and LUMO levels functions as an indicator of the chemical reactivity of the compounds, with a lower ΔE value indicating higher reactivity. The predicted energy gap values in Table 2 confirm that all investigated compounds within the (ATNM)n series share

similar reactivity. Furthermore, the designed homologues (ATNM)n displays analogous electron cloud distributions over the carbon atoms, the π-system of the azomethine linkage, and the thiazole ring.

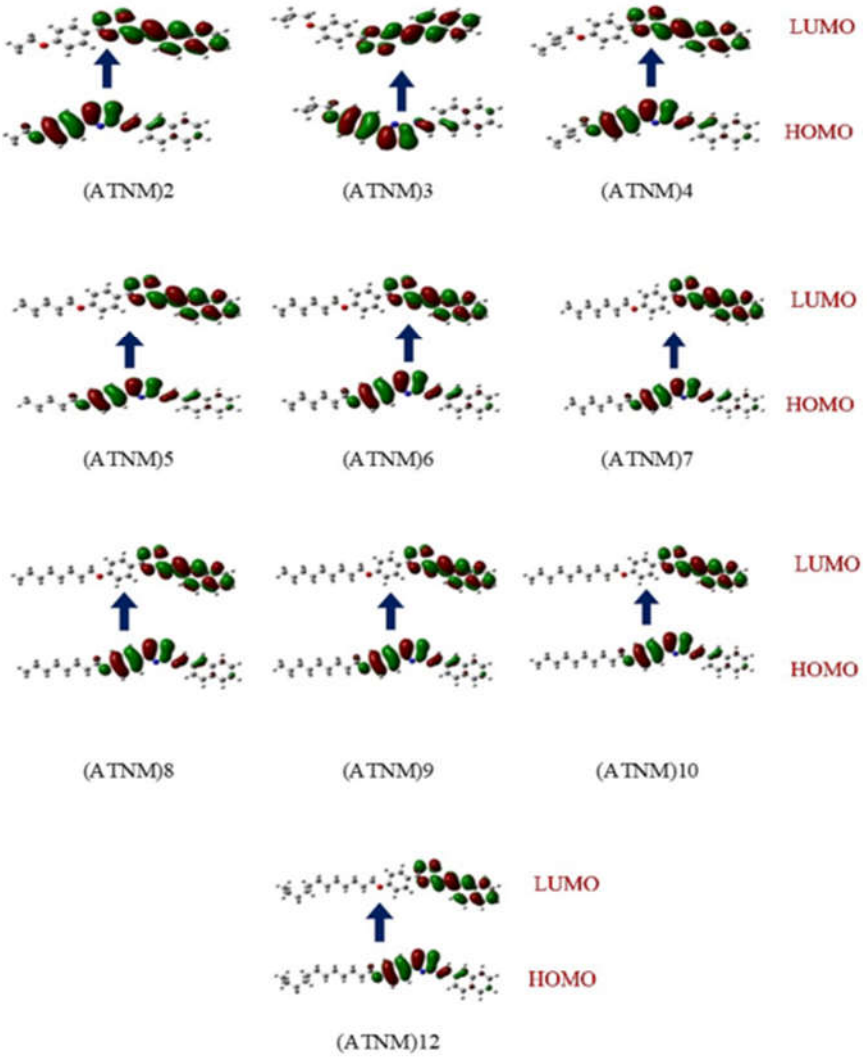

Figure 6. The computed diagrams depict the frontier molecular orbitals for the synthesized compounds (ATNM)n.

Molecular electrostatic potential (MEP)

MEP serves as an indicator, revealing the distribution of electron density within the molecular structure [35]. Employing the DFT/B3LYP methods and a 6-311G (d,p) basis sets, the charge

distribution map for the synthesized compounds (ATNM)n was calculated, following the principles of molecular electrostatic potential (MEP) as depicted in Figure 7.

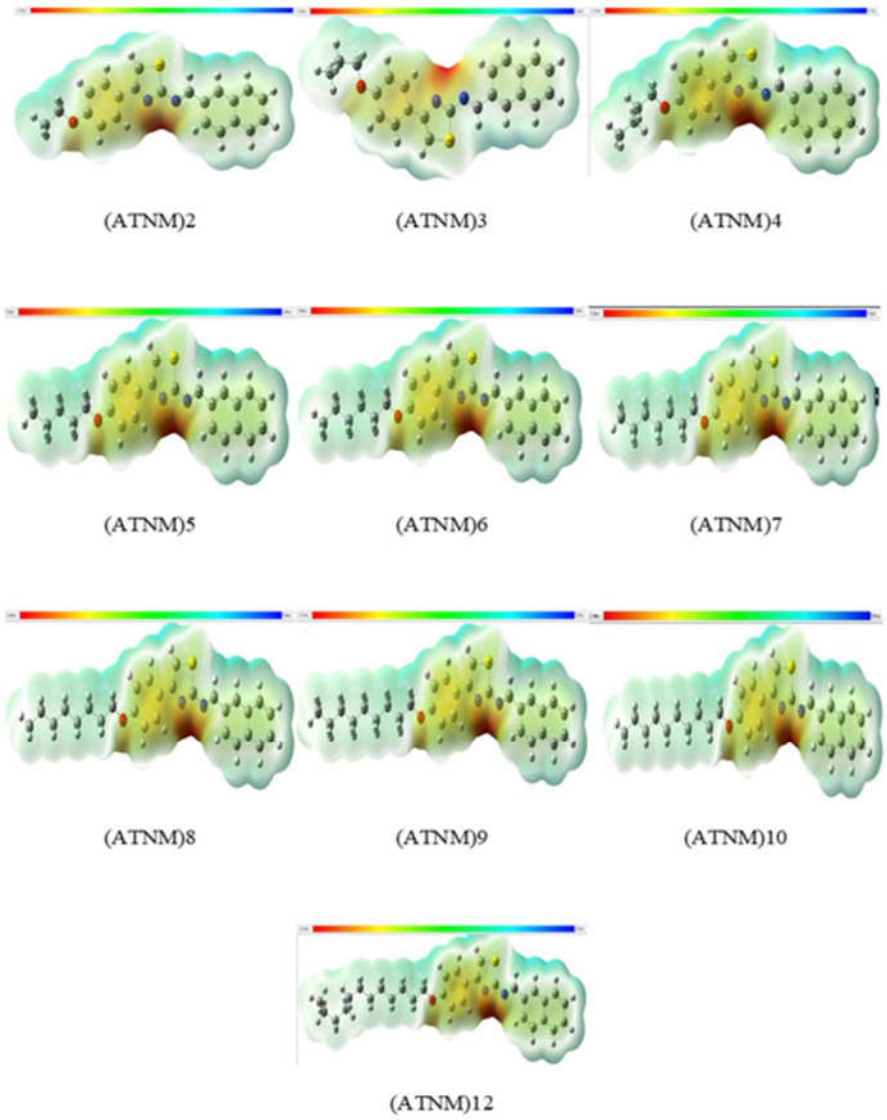

Figure 7. MEP for the synthesized (ATNM)n compounds.

MEP stands out as one of the most effective approaches for discerning both intermolecular and intramolecular interactions within a substance. In the (ATNM)n compounds, the presence of the polar N atom and the connecting CH=N group influenced the localization of iso-electronic density in regions with varying electron richness [36]. Specifically, the CH=N group in the Schiff base segment represents the most electron-deficient site, while the terminal alkoxy chain

constitutes the most electron-rich region. The areas highlighted in red indicate the most negatively charged sites, attributed to the presence of highly electronegative oxygen atoms, while the regions colored in blue represent the most positively charged areas. An observation was made that the negative charge is localized at a considerable distance from the center of the (ATNM)n compounds, which might offer an explanation for the absence of the liquid crystalline phase as mentioned in [37].

CONCLUSIONS

In this study, we synthesized and examined a novel set of compounds incorporating thiazole, azomethine, and naphthalene components, denoted as N-(4-(4-Alkoxyphenyl) thiazol-2-yl)-1-(naphthalen-2-yl) methanimine (ATNM)n, where the alkoxy chain varied in length ($C_nH_{2n+1}O$, n = 2, 3, 4, 5, 6, 7, 8, 9, 10, and 12). The synthesis of these compounds was successfully accomplished, and the proposed structures were verified through FT-IR, ^{1}H NMR, ^{13}C NMR analyses. Additionally, their optical and thermal characteristics were assessed using optical polarizing microscopy (POM) and differential scanning calorimetry (DSC). Notably, none of the members within this series exhibited mesomorphic properties typical of liquid crystals.

The DFT analyses were conducted to illustrate the non-planar geometry in all studied compounds. The twist angle of CH=N is observed to be influenced by the level of conjugation and the thiazole component's contribution and the length of the terminal chain enhanced the geometrical parameters. Furthermore, the predicted charge distribution maps could serve as a tool to elucidate the reasons for the absence of liquid crystal characteristics in the synthesized compounds.

ACKNOWLEDGEMENTS

The authors express gratitude to the Department of Chemistry, Faculty of Science and Health, at Koya University, Iraq, and the Department of Petroleum Technology - Chemical Analysis, Koya Technical Institute, at Erbil Polytechnic University, Iraq, for their assistance and support in providing the essential laboratory facilities and necessary instruments for this research.

REFERENCES

1. Zewdie, H., Meanfield theory of the nematic liquid crystal free surface. *Bull. Chem. Soc. Ethiop*. **1989**, 3, 121-127.
2. Newkome, G.; Hager, D. Chemistry of heterocyclic compounds. 27. An improved preparation of pyridyldiphenylphosphines. *J. Org. Chem*. **1978**, 43, 947-949.
3. Karamysheva, L.; Kovshev, E.; Pavluchenko, A.; Roitman, K.; Titov, V.; Torgova, S.; Grebenkin, M.; Crystals, L. New heterocyclic liquid crystalline compounds. *Mol Cryst. Liq. Cryst*. **1981**, 67, 241-251.
4. Lee, C.-H.; Yamamoto, T.; Science, L.; Crystals, T.; Crystals, L. Synthesis of liquid crystals with bent-rod structure: mesogenic thiazole derivatives with long alkoxyl chains. *Mol. Cryst. Liq. Cryst.* **2001**, 363, 77-84.
5. Alwan, E.S.; Mohareb, R.M. Synthesis of bioactive heterocyclic compounds using camphor. *Bull. Chem. Soc. Ethiop*. **2024**, 38, 1069-1076.
6. Egan, R.; Tadanier, J.; Garmaise, D.; Gaunce, A. Intermediates in the Hantzsch thiazole synthesis. *J. Org. Chem.* **1968**, 33, 4422-4426.
7. Mallia, C.J.; Englert, L.; Walter, G.C. Thiazole formation through a modified Gewald reaction. *Beilstein J. Org. Chem.* **2015**, 11, 875-883.
8. Gaikwad, N.; Patil, S.; Bobade, V. Synthesis and antimicrobial activity of novel thiazole substituted pyrazole derivatives. *J. Heterocycl. Chem*. **2013**, 50, 519-527.

9. Titov, V.; Pavlyuchenko, A. Thermotropic liquid crystals in the heterocyclic series. *Beilstein J. Org. Chem.* **1980**, 16, 1-13.
10. Murza, M.; Kuvatov, Z.K.; Safarov, M. Geometry and mesomorphic properties of new Schiff bases containing thiazole ring. *Chem. Heterocycl. Comp.* **1999**, 35, 1097-1103.
11. Murza, M.; Prosochina, T.; Safarov, M.; Kantor, E. Synthesis and quantum-chemical study of liquid-crystal derivatives of thiazole. *Chem. Heterocycl. Comp.* **2001**, 37, 1258-1265.
12. Dodson, R.M.; King, L.C. The reaction of acetophenone with thiourea and oxidizing agents. *J. Am. Chem. Soc*. **1946**, 68, 871-871.
13. Karam, N.H.; Tomma, J.H.; Al-Dujaili, A.H. Synthesis and characterization of new derivatives of thiazole with liquid crystalline properties. *Chem. Mater. Res.* **2013**, 3, 162-171.
14. Mamad, D.M.; Rasul, H.H.; Awla, A.H.; Omer, R.A. *Insight into Corrosion Inhibition Efficiency of Imidazole-Based Molecules: A Quantum Chemical Study* in *Doklady Physical Chemistry*, Vol. 511, Pleiades Publishing Ltd.: State of Delaware, USA; **2023**; pp. 125-133.
15. Parlak, A.E.; Omar, R.A.; Koparir, P.; Salih, M. Experimental, DFT and theoretical corrosion Study for 4-(((4-ethyl-5-(thiophen-2-yl)-4H-1, 2, 4-triazole-3-yl) thio) methyl)-7, 8-dimethyl-2H-chromen-2-one. *Arab. J. Chem*. **2022**, 15, 104088.
16. Steinmann, S.N.; Corminboeuf, C.J. Exploring the limits of density functional approximations for interaction energies of molecular precursors to organic electronics. *J. Chem. Theory Comput.* **2012**, 8, 4305-4316.
17. Rasul, H.H.; Mamad, D.M.; Azeez, Y.H.; Omer, R.A.; Omer, K.A. Theoretical investigation on corrosion inhibition efficiency of some amino acid compounds. *Comput. Theoret. Chem*. **2023**, 1255, 114-177.
18. Vogel, I. *A Textbook of Practical Organic Chemistry*, 5th ed., John Wiley and Sons, Inc.: New York; **1989**; p 309.
19. Rao, V.K.; Reddy, S.S.; Krishna, B.S.; Naidu, K.R.; Raju, C.N.; Ghosh, S.K. Synthesis of Schiff's bases in aqueous medium: A green alternative approach with effective mass yield and high reaction rates. *Green Chem. Lett. Rev.* **2010**, 3, 217-223.
20. Brown, H.W.; Foote, S.C. *Organic Chemistry*, 3rd ed., Thomson Learning Academic Resource Center: USA; **2002**; p 395-396.
21. Busch, K.W.; Wang, H.; Small, G.W.; Fountain III, A.W. *Book Review: Handbook of Near-Infrared Analysis, Infrared and Raman Characteristic Group Frequencies: Table and Charts, Mass Spectrometry Principles and Applications, Mass Spectrometry Principles and Applications, NMR Spectroscopy: Data Acquisition, Fourier Transforms in Spectroscopy, Handbook of Raman Spectroscopy*, 3rd ed., SAGE Publications Sage UK: London, England **2002**; p 189-190.
22. Sasaki, S.-I.; *Handbook of Proton-NMR Spectra and Data*, Vol. 1, Academic Press: UK; **1985**.
23. Johnson Jr, C.; Bovey, F. Calculation of nuclear magnetic resonance spectra of aromatic hydrocarbons. *J. Chem. Phys*. **1958**, 29, 1012-1014.
24. Xue, W.J.; Zheng, K.L.; Li, H.Z.; Gao, F.F.; Wu, A.X. Iodine-promoted selective synthesis of substituted aminothiazole via a self-sorting reaction network. *Tetrahedron Lett.* **2014**, 55, 4212-4215.
25. McMurry, J.; Simanek, E. *Fundamentals of Organic Chemistry*, 6th ed., Thomson Brooks: Cole; **2007**, p 243-244.
26. Thompson, J.M. *Infrared Spectroscopy*, 1st ed., Jenny Stanford Publishing: New York; **2018**; p 88-89.
27. Ferrari, M.; Mottola, L.; Quaresima, V. Principles, techniques, and limitations of near infrared spectroscopy. *Canad. J. Appl. Physiol*. **2004**, 29, 463-487.
28. Ott, J.B.; Boerio-Goates, J. *Chemical Thermodynamics: Advanced Applications: Advanced Applications*, Academic Press: United Kingdam; **2000**; p 75.
29. Brown, G.; Wolken, J.J. *Liquid Crystals and Biological Structures*, Academic Press: United Kingdam; **1979**; p 47.

30. Dierking, I. *Textures of Liquid Crystals*. Wiley VCH Veriage: United Kingdam, Manchester; **2003**; p 52.
31. Fleischmann, E.K.; Zentel, R.J. Liquid-crystalline ordering as a concept in materials science: From semiconductors to stimuli-responsive devices. *J. German Chem. Soc*. **2013**, 52, 8810-8827.
32. Dave, J.; Kurian, G.; Prajapati, A.; Vora, R.; Crystals, L. Mesomorphic behaviours of Schiff's base compounds: I: N,N′-Di (4-n-alkoxy-l-naphthylidene)-benzidines. *Mol. Cryst. Liq. Cryst.* **1971**, 14, 307-317.
33. Dave, J.; Kljrian, G.; Prajapati, A.; Crystals, L. Influence of naphthalene moiety on mesomorphism. *Mol. Cryst. Liq. Cryst.* **1983**, 99, 385-389.
34. Ahmed, H.; El-Atawy, M.J. Synthesis, mesomorphic and geometrical approaches of new non-symmetrical system based on central naphthalene moiety. *Angew. Chem. Int. Ed.* **2021**, 48, 1940-1952.
35. Scrocco, E.; Tomasi, J. Electronic molecular structure, reactivity and intermolecular forces: An euristic interpretation by means of electrostatic molecular potentials. *Adv. Quantum Chem*. **1978**, 9, 115-193.
36. Marks, T.; Ratner, M.A. Design, synthesis, and properties of molecule-based assemblies with large second-order optical nonlinearities. *Angew. Chem. Int. Ed. Eng.* **1995**, 34, 155-173.
37. Soni, R.; Nakum, K.J.; Katariya, K.D.; Soman, S.S.; Nada, S.; Hagar, M.J. Synthesis, mesomorphic properties and DFT calculations of new coumarin Schiff base-ester. *Liq. Cryst.* **2023**, 50, 636-651.